

Natural convection in partially cooled and inclined porous rectangular enclosures

Hakan F. Oztop *

Department of Mechanical Engineering, Firat University, 23119 Elazig, Turkey

Received 4 October 2005; received in revised form 22 April 2006; accepted 24 April 2006

Available online 8 June 2006

Abstract

Natural convection heat transfer in a partially cooled and inclined rectangular enclosure filled with saturated porous medium has been investigated numerically. One of side wall has constant hot temperature and one adjacent wall is partially cooled while the remaining ones are adiabatic. Finite volume based finite difference method was applied using the SIMPLE algorithm. Governing parameters are Darcy Rayleigh number ($10 \leq Ra \leq 1000$), center of location of heater ($0.1 \leq c \leq 0.9$), inclination angle ($0^\circ \leq \phi \leq 90^\circ$) and length of cooler ($0.25 \leq w \leq 0.75$). It is found that inclination angle is the dominant parameter on heat transfer and fluid flow as well as aspect ratio.

© 2006 Elsevier Masson SAS. All rights reserved.

Keywords: Porous medium; Inclination angle; Natural convection heat transfer

1. Introduction

Thermally driven flows in porous media have received a great deal of attention because of the increasing interest in engineering applications such as geothermal energy systems, compact heat exchangers, nuclear engineering, cooling of radioactive waste containers etc.

In the open literature, there are very large number of papers about thermally driven flows with rectangle or square (horizontal or inclined) porous enclosure differentially heated sidewalls and insulated bottom and ceiling [1–5]. Besides, Prasad and Kulacki [6], Sen et al. [7], Baytas and Pop [8], Nithiarasu et al. [9], Moya et al. [10], Al-Amiri [11], Lauriat and Prasad [12], Saeid and Pop [13], have made numerical studies to investigate the phenomenon in differentially heated enclosures. In all studies, entire wall has constant temperature or adiabatic.

The number of partially heated and cooled porous or non-porous enclosures are very limited even though they find a wide application area such as in flush mounted electronical heater or buildings. Partially heated or cooled non-porous enclosures were studied by Farouk and Fusegi [14], Chu and Hickox [15],

Oztop et al. [16], Oztop [17], Aydin and Yang [18], Turkoglu and Yucel [19], Chu et al. [20]. About the partially heated or cooled porous medium, Prasad and Kulacki [21] made a numerical solution of the natural convection equations for porous cavity partially heated from bottom wall. They used the Darcy law to simulate heat transfer and flow field and investigated the location of heater with a different aspect ratio of the cavity. They showed that a plume-like flow occurs above the heated region with the increasing of Rayleigh number. El-Refaee et al. [22] applied the fast false implicit transient scheme (FITS) algorithm to simulate natural convection in a tilted and partially cooled rectangular enclosure filled with non-porous medium. Their results show that both aspect ratio and inclination angle have significant effect on natural convection heat transfer. Recently, Bourich et al. [23] made a numerical analysis of the double-diffusive natural convection in a porous enclosure partially heated from below. They indicated that dimensionless position of the heating element plays important role on flow regime with different Lewis and Rayleigh numbers.

Other important parameter on natural convection in cavities is aspect ratio, as indicated by Frederick [24]. Also, this parameter is important for cavities filled with porous medium. In this context, Vasseur et al. [25] analyzed the natural convection both numerically and analytically in an inclined porous rectan-

* Tel.: +90 424 237 0000 ext. 5328; fax: +90 424 241 5526.

E-mail address: hfoztop1@yahoo.com (H.F. Oztop).

Nomenclature

A	aspect ratio, L/H	x, y	coordinate axes
c	center of location of heater		
C	specific heat $\text{J kg}^{-1} \text{K}^{-1}$		
C_F	Forcheimer number		
d	particle diameter m		
Da	Darcy number		
g	gravity m s^{-2}		
Gr	Grashof number		
H	cavity height m		
K	permeability m^2		
L	cavity length m		
Nu	local Nusselt number		
Pr	Prandtl number		
p	pressure N m^{-2}		
Ra	Rayleigh number		
T	temperature K		
u, v	velocities m s^{-1}		
w	length of cooler		
			<i>Greek symbols</i>
		β	thermal expansion coefficient 1 K^{-1}
		ε	porosity
		ϕ	inclination angle
		ρ	density kg m^{-3}
		ψ	Streamfunction
		ν	kinematic viscosity $\text{m}^2 \text{ s}^{-1}$
			<i>Subscript</i>
		c	cold
		h	hot
		f	fluid
		i, j	spatial indices
		m	mean
			<i>Superscript</i>
		'	non-dimensional quantities

gular cavity subject to constant heat flux. Hossain and Rees [26] made a numerical solution to investigate Darcy–Benard convection problem in a rectangular cavity which was heated from below and had with cold sidewalls. They demonstrated that the flow becomes weaker as the Darcy number decreases from the pure fluid limit towards the Darcy-flow limit. Robillard et al. [27] studied multiple steady states in a confined porous medium with localized heating from below using a numerical technique.

To the best of the authors' knowledge, the natural convection heat transfer in inclined partially cooled porous cavity from one wall has not yet been investigated. The main aim of the study is to examine laminar natural convection flow and heat transfer in a porous enclosure using the parameters as Rayleigh number, inclination angle, aspect ratio and locations of the cooler.

2. Physical model

Schematic configuration of the rectangular ($H \times L$) enclosure can be seen in Fig. 1. It is filled with fluid saturated porous medium. The cavity is partially cooled at a constant temperature from one wall while its left entire wall has hot temperature and the others are adiabatic. All walls of the cavity are assumed to be impermeable. ϕ , denotes the inclination angle of the enclosure with respect to the horizontal plane. Also, stratification and local thermal non-equilibrium is neglected in the present study. The distance between the center of the cooler and vertical wall is depicted by c and w , is the length of cooler which is taken as 0.5 for the sake of a shorter paper.

3. Computational details

In this study, fluid is assumed as Newtonian, incompressible and the flow is laminar. Also, thermophysical properties

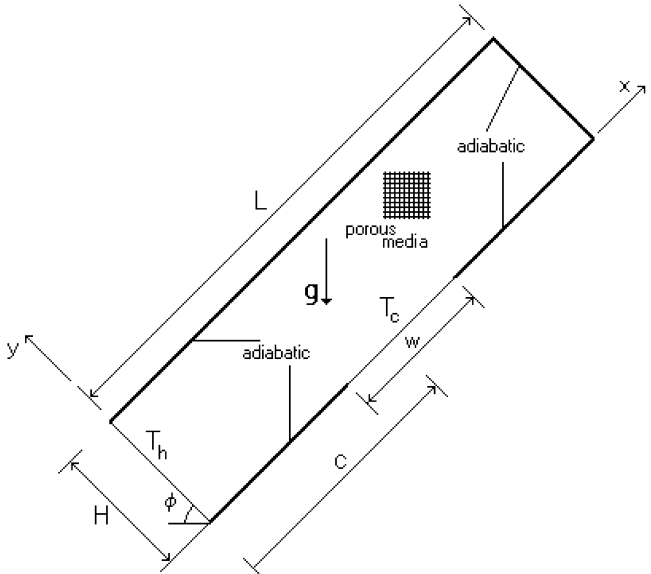


Fig. 1. Rectangular inclined partially cooled enclosure.

of fluid are constant. Boussinesq approximation is applied and initial effects are neglected. Also, it is assumed that porosity and permeability of the homogeneous porous medium are uniform and the saturated porous medium is assumed to be isotropic in thermal conductivity. General equation of continuity, momentum and energy in Cartesian coordinates are written as (Nakayama [28]),

$$\frac{\partial u_j}{\partial x_j} = 0 \quad (1)$$

$$\frac{1}{\varepsilon} \frac{\partial}{\partial x_j} \left\{ u_j u_i - (\varepsilon \nu) \frac{\partial u_i}{\partial x_j} \right\}$$

$$= -\frac{\varepsilon}{\rho_f} \frac{\partial p}{\partial x_i} + \varepsilon g_i \beta (T - T_{ref}) c_x + \frac{\partial}{\partial x_j} (v) \frac{\partial u_j}{\partial x_i} - \frac{1}{\varepsilon} \left\{ \frac{(\varepsilon v)}{(K/\varepsilon)} + \frac{C_F}{(K/\varepsilon)^{1/2}} (u_j u_j)^{1/2} \right\} u_i \quad (2)$$

$$\frac{\partial}{\partial x_j} \left\{ u_j T - \frac{v}{Pr} \frac{\partial T}{\partial x_j} \right\} = \frac{S}{\rho_f C_p} \quad (3)$$

The dimensionless form of the governing equations can be obtained as given below:

Continuity

$$\frac{\partial u'}{\partial x'} + \frac{\partial v'}{\partial y'} = 0 \quad (4)$$

x-momentum

$$\begin{aligned} \frac{1}{\varepsilon} u' \frac{\partial}{\partial x'} \left(\frac{u'}{\varepsilon} \right) + v' \frac{\partial v'}{\partial y'} \left(\frac{u'}{\varepsilon} \right) \\ = -\frac{1}{\varepsilon} \frac{\partial}{\partial x'} (\varepsilon p') - \frac{Pr}{Da} u' - C_F \frac{(u'^2 + v'^2)^{1/2}}{\sqrt{Da}} \frac{u'}{\varepsilon^{3/2}} \\ + \frac{Pr}{\varepsilon} \left(\frac{\partial^2 u'}{\partial x'^2} + \frac{\partial^2 u'}{\partial y'^2} \right) + Ra Pr T' \cos \phi \end{aligned} \quad (5)$$

y-momentum

$$\begin{aligned} \frac{1}{\varepsilon} u' \frac{\partial}{\partial x'} \left(\frac{v'}{\varepsilon} \right) + v' \frac{\partial v'}{\partial y'} \left(\frac{v'}{\varepsilon} \right) \\ = -\frac{1}{\varepsilon} \frac{\partial}{\partial y'} (\varepsilon p') - \frac{Pr}{Da} v' - C_F \frac{(u'^2 + v'^2)^{1/2}}{\sqrt{Da}} \frac{v'}{\varepsilon^{3/2}} \\ + \frac{Pr}{\varepsilon} \left(\frac{\partial^2 v'}{\partial x'^2} + \frac{\partial^2 v'}{\partial y'^2} \right) + Ra Pr T' \sin \phi \end{aligned} \quad (6)$$

Energy

$$u' \frac{\partial T'}{\partial x'} + v' \frac{\partial T'}{\partial y'} = \frac{\partial^2 T'}{\partial x'^2} + \frac{\partial^2 T'}{\partial y'^2} \quad (7)$$

where the following scales have been used for non-dimensionalisation

$$\begin{aligned} x' = \frac{x}{H}, \quad y' = \frac{y}{H}, \quad u' = \frac{u}{v/H}, \quad v' = \frac{v}{v/H} \\ p' = \frac{p}{\rho v/H^2}, \quad T' = \frac{T - T_c}{T_h - T_c}, \quad Da = \frac{K}{H^2} \\ Gr = \frac{g \beta \Delta T H^3}{v^2} \quad Pr = \frac{v}{\alpha}, \quad Ra = Gr Pr Da \end{aligned} \quad (8)$$

The geometric function C_F (Forcheimer number) and the permeability of the porous medium K are based on Ergun's empirical expression (Ergun [29]), which may be used for the packed beds that may be closely modeled as spherical beads of diameter, d , as (Nakayama [28], Al-Amiri [11] and Narasimhan and Lage [31]).

$$K = \frac{\varepsilon^3 d^2}{150(1-\varepsilon)^2} \quad (9)$$

$$C_F = \frac{1.75}{(150\varepsilon^3)^{1/2}} \quad (10)$$

The porosity, ε is assumed uniform throughout the enclosure ($\varepsilon = 0.9$) which represents the high porosity medium.

Table 1
Comparison of mean Nusselt numbers with literature

Study	Nu_m for $Ra = 10^2$
Baytas [32]	3.160
Saeid and Pop [33]	3.002
Present	2.980

According to physical model of Fig. 1, boundary conditions for the problem are $u = v = 0$ for all walls

$$T = T_h \quad \text{at } x' = 0 \quad (11)$$

$$T = T_c \quad \text{at } c - w/2 < x' < c + w/2 \text{ and} \\ y' = 0 \text{ and the others } \frac{\partial T'}{\partial y'} = 0 \quad (12)$$

$$\frac{\partial T'}{\partial y'} = 0 \quad \text{at } y' = H \quad (13)$$

$$\frac{\partial T'}{\partial x'} = 0 \quad \text{at } x' = L \quad (14)$$

The calculation of Mean Nusselt number is obtained via Eq. (16),

$$Nu = -\left. \frac{\partial T'}{\partial x'} \right|_{x=0} \quad (15)$$

$$Nu_m = -\int_0^1 Nu dy' \quad (16)$$

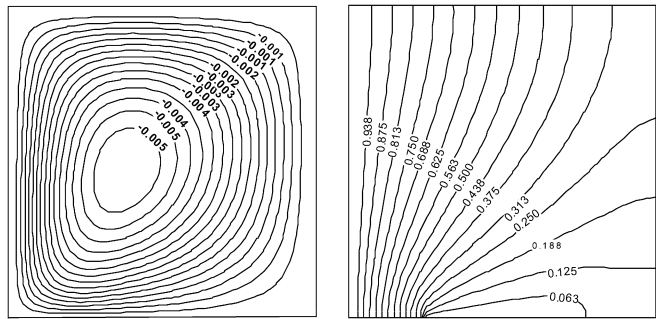
The stream function is calculated from its definition as

$$u' = \frac{\partial \psi}{\partial y'}, \quad v' = -\frac{\partial \psi}{\partial x'} \quad (17)$$

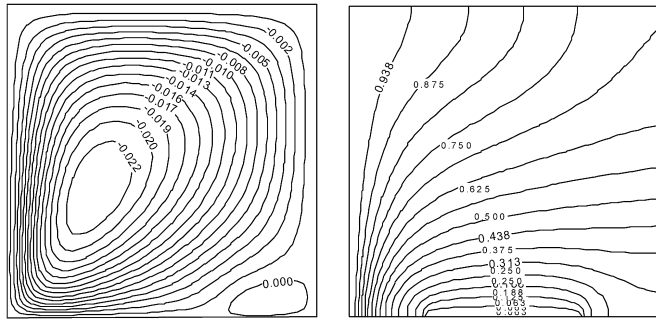
Finite volume based finite difference method is used to solve the governing equation using staggered grid arrangement. Modified version according to present study of the general purpose of SAINTS (Software for arbitrary integration of Navier–Stokes equation with Turbulence and Porous Media Simulator) code, proposed by Nakayama [28], is used. Patankar's SIMPLE solution algorithm by Patankar [30] is used in the code. A hybrid of the central difference and upwind schemes was used for the convective and diffusive terms. Solution of linear algebraic equation is made by TDMA (Three Diagonal Matrix Algorithm). An under-relaxation parameter of 0.3, 0.3, 0.2 and 0.5 were used in order to obtain a stable convergence for the solution of u -velocity, v -velocity, pressure and energy equations. In this study, uniform mesh sizes are used and 48×48 grids are chosen for the grid arrangement and it is found that this grid solution is enough. The validation of the present code was made with the previously published paper for differentially heated enclosure as listed in the Table 1. As can be shown from the table that results shows good agreement with the literature.

4. Results and discussion

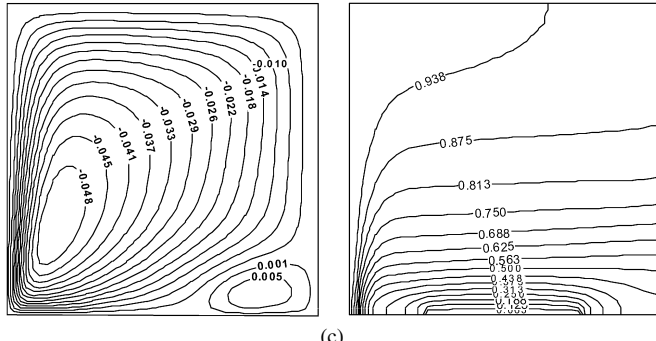
A numerical study was performed to examine the steady-state, laminar natural convection heat transfer in an inclined rectangular porous enclosure with the parameters as Darcy



(a)



(b)

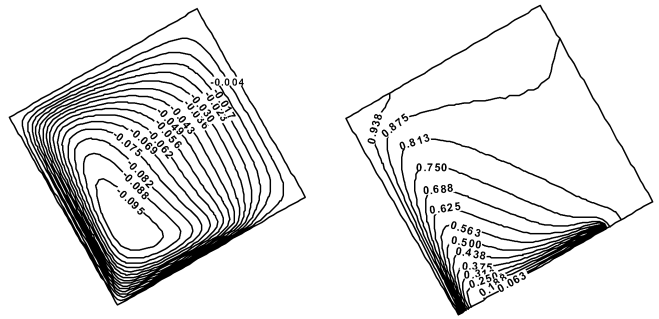


(c)

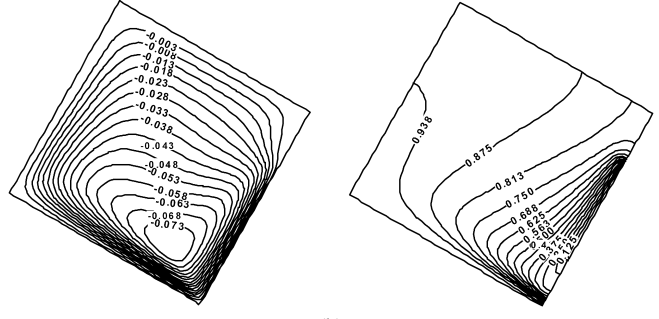
Fig. 2. Streamline and isotherm for $A = 1$, $c/L = 0.5$, $w/L = 0.5$ and $\phi = 0^\circ$
(a) $Ra = 10$, (b) $Ra = 100$, (c) $Ra = 1000$.

Rayleigh number (10–1000), inclination angle (0° – 90°), location (0.1–0.9) and length of cooler. Prandtl number is taken as $Pr = 1$. The author is not aware of any existing experimental data with which to compare the numerical results.

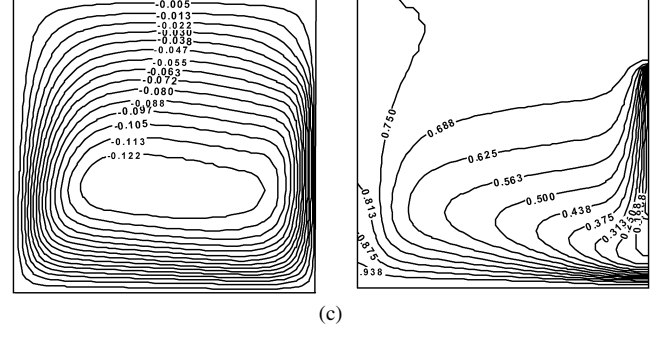
Streamlines and isotherms are plotted in Figs. 2–5 to obtain flow patterns and temperature fields at different Rayleigh numbers such as $Ra = 10$, 100 and 1000 for $A = 1$ and $\phi = 0^\circ$, which refer the horizontal enclosure. Fig. 2 illustrates them for $Ra = 10$ which is the smallest Rayleigh number in the present study. In Fig. 2(a), a single cell is obtained in the clockwise direction and its center come closer to the right bottom corner of the enclosure as Ra number increases. Also, another cell arises at the right bottom corner in counterclockwise direction for $Ra > 100$ and its length increases with increasing Rayleigh number. However, conduction temperature fields are dominated for lower Ra number as indicated in isotherms in Fig. 2(a) due to stronger influence of the entire heated wall as indicated by Prasad and Kulacki [6]. But when Rayleigh number is increased, convection heat transfer becomes stronger. As indicated in Fig. 2(c), the disturbance in the temperature field is



(a)



(b)



(c)

Fig. 3. Streamline and isotherms at various inclination angle ($\phi = 30^\circ$, 60° , 90°) for $Ra = 1000$, $c/L = 0.5$, $w/L = 0.5$ and $A = 1$.

mostly near the cold surface and with the increasing of Rayleigh number, the isotherms move toward to the partially cold surface.

Inclination angle is an important parameter for some engineering problems. Fig. 3 presents the isotherms and streamlines for $Ra = 1000$ and $A = 1$ to show the effect of inclination angle. Smaller Rayleigh number and inclination angle is chosen to prevent instability problem. Three different inclination angles (ϕ) are tested between 30° and 90° . When the inclination angle is chosen as 30° instead of 0° as indicated in Fig. 2(c), both flow field and temperature distribution are affected from the inclination angle and single cell is obtained in Fig. 3(a). Its length is smaller for $\phi = 60^\circ$ as indicated in Fig. 3(b). Also, disturbance in the temperature field is mostly near the hot vertical wall for $\phi = 60^\circ$. Fig. 3(c) shows the streamline and isotherm for $\phi = 90^\circ$. It means that, entire bottom surface is heated and right vertical wall is cooled. In this case, again a single cell in clockwise direction was formed but its length becomes very big. In Figs. 4(a)–(c), the temperature and flow fields are presented for different aspect ratios of $A = 1$, 3 and 5 for $Ra = 1000$ and

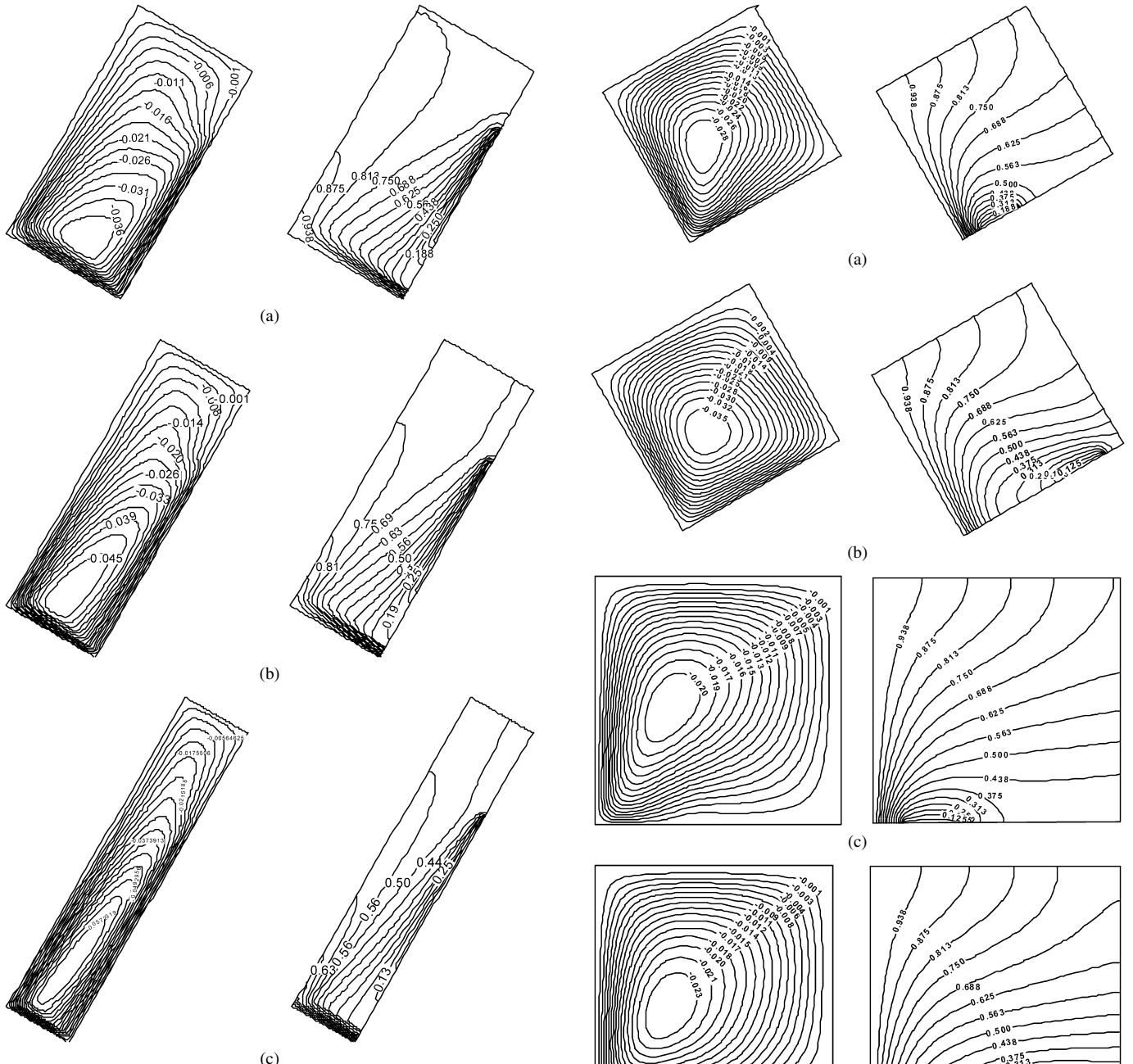


Fig. 4. Streamlines and isotherms for various aspect ratio (a) $A = 2$, (b) $A = 3$, (c) $A = 5$ for $Ra = 1000$, $c/L = 0.5$, $w/L = 0.5$ and $\phi = 60^\circ$.

$\phi = 60^\circ$. The enclosure swallows from Fig. 4(a) to Fig. 4(c). As can be shown from the streamlines that smaller cell is obtained for higher aspect ratio of the cavity. In other words, this cell becomes longer as aspect ratio increases because of the narrow cavity. It can be argued that the role of aspect ratio is the dominant factor for other constant parameters as indicated by Prasad and Kulacki [6]. In this case, conduction heat transfer is the dominant factor to convection as can be seen from the isotherm and a cold region is formed at the right corner of the cavity especially at the value of aspect ratio is $A = 3$ and 5 . The effect of location (c/L) of cooler is given in Fig. 5 for $A = 1$ and $Ra = 100$. In this figure, two different locations of cooler are plotted for two different inclination angles. Length

Fig. 5. Streamlines and isotherms at different locations of cooler for $A = 1$ and $Ra = 100$ (a) $\phi = 30^\circ$, $c/L = 0.25$ and $w/L = 0.5$, (b) $\phi = 30^\circ$, $c/L = 0.75$ and $w/L = 0.5$, (c) $\phi = 0^\circ$, $c/L = 0.25$ and $w/L = 0.25$, (d) $\phi = 0^\circ$, $c/L = 0.75$ and $w/L = 0.25$.

of the cooler is equal for all cases at $w/L = 0.5$. In this context, figures (a) and (b) shows streamlines and isotherms for $\phi = 30^\circ$, $c/L = 0.25$ and $c/L = 0.75$, respectively. In both cases, single cell is formed in the clockwise direction but as cooler location is moved to right vertical wall ($c/L = 0.75$) smaller streamfunction value is obtained as can be seen from the figures. Also, its center goes to center of the enclosure in the case of $c/L = 0.75$. This is because of the longer distance between heater and cooler. Also, as can be seen from the Fig. 5(b),

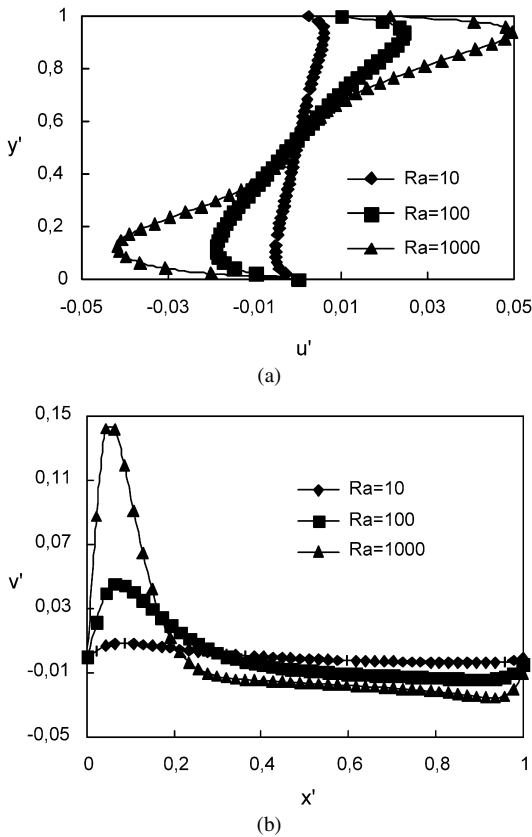


Fig. 6. Velocity profiles (a) along x -axes, (b) along y -axes.

heat transfer is not strong again because of the long distance. Conduction heat transfer mode is effective near the cooler and parallel isotherms are formed. If inclination angle is chosen as $\phi = 0^\circ$, the value of streamfunction of main cell is almost the same. But in this case, a very small second cell, which is not plotted in the figure, appears.

Velocity components along x - and y -axes are plotted for different Ra number at $A = 1$ and $\phi = 0^\circ$ in Fig. 6. Velocities are plotted at the middle of the enclosure, $x = 0.5$, and $y = 0.5$ for axial and radial velocities, respectively. As can be seen from the figure, velocities increase with increasing Rayleigh numbers. As indicated in Fig. 6(a), for small Rayleigh numbers velocities are symmetric but for higher Rayleigh numbers asymmetric axial velocity profiles are formed due to asymmetric heating. The velocity of flow is higher at the upper half of the cavity than that of bottom half. But for the radial velocity profiles (Fig. 6(b)), velocity is higher near the hot vertical wall and it decreases continually with an increase in the horizontal distance.

Variation of local Nusselt number along the heat wall is given in Fig. 7 for different parameters. Fig. 7(a) gives the local Nusselt number for $Ra = 100$ and $\phi = 0^\circ$ for different aspect ratio of the enclosure. Its value is decreased from bottom to top. This is because of lower convective velocity on the top wall of the enclosure. As indicated in the figure that as aspect ratio is increased the value of local Nusselt number is decreased since heat transfer per unit area is decreased as aspect ratio increased as indicated Prasad and Kulacki's [6] study. Fig. 7(b) is plotted to see the effect of inclination angle at the same Ra

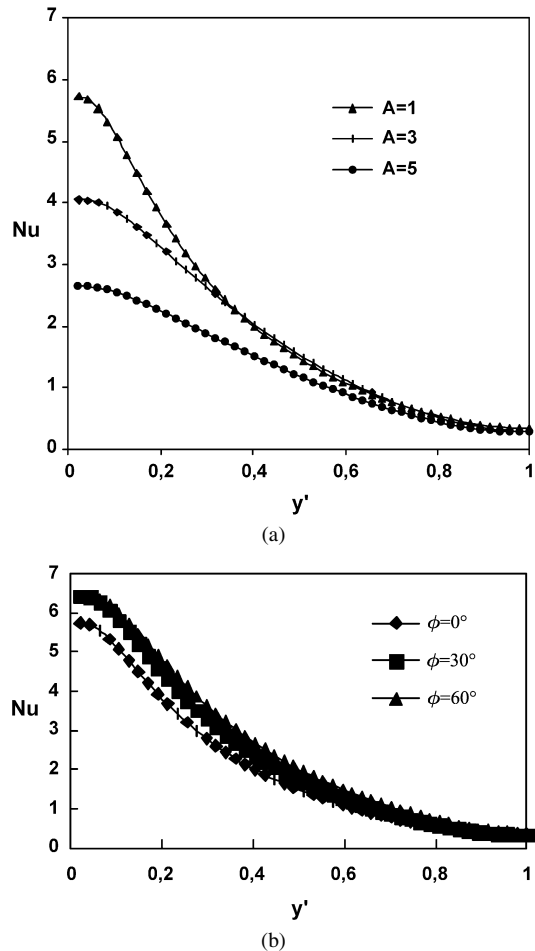


Fig. 7. Variation of local Nusselt number along the heat wall (a) $\phi = 0^\circ$ and $Ra = 100$ for different aspect ratio, (b) $Ra = 100$ and $A = 1$ for different inclination angle.

number and for $A = 1$. In this figure, the lowest value is formed for $\phi = 0^\circ$. Also, values are very close to case of $\phi = 30^\circ$ and $\phi = 60^\circ$. But the highest one is obtained for $\phi = 60^\circ$. Inclination angle is effective especially at the bottom of the enclosure. Fig. 8 shows the variation of mean Nusselt number for different aspect ratios. Mean Nusselt number is calculated along the heated vertical wall. It is given for $c/L = 0.5$, $w/L = 0.5$ and $\phi = 30^\circ$. As can be seen from the figure, the highest Nusselt number is obtained for and the lowest aspect ratio. Mean Nusselt values are increased almost linearly with the increasing of Rayleigh number. However, their values are decreased as aspect ratio increased. Computational results of Prasad and Kulacki [22] for partially heated from the bottom wall support this observation. Because, heat source is loosed more and more energy when the end walls are moved away from the leading edge of the heated segment.

Variations of local Nusselt number along the heated wall for different aspect ratio of enclosure and different location of partially cooler are presented in Fig. 9 at $Ra = 100$, $w/L = 0.25$ and $\phi = 60^\circ$. As indicated in the figure, values of local Nusselt numbers are decreased toward to maximum height of heated wall. Also, it is decreased with the increasing of location of cooler due to increasing distance between hot and cold walls.

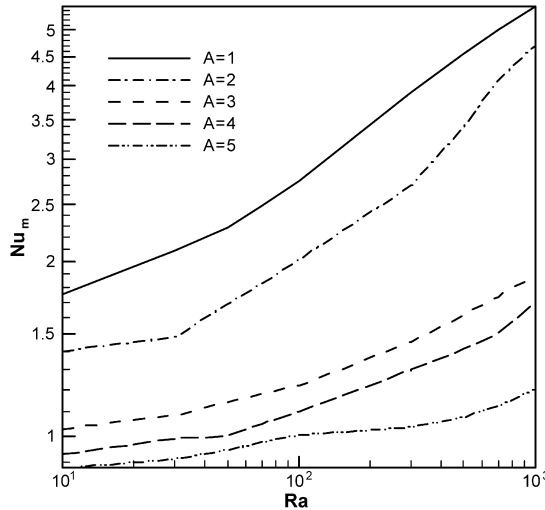


Fig. 8. Variation of mean Nusselt number with Rayleigh number for different aspect ratio for $c/L = 0.5$, $w/L = 0.5$ and $\phi = 30^\circ$.

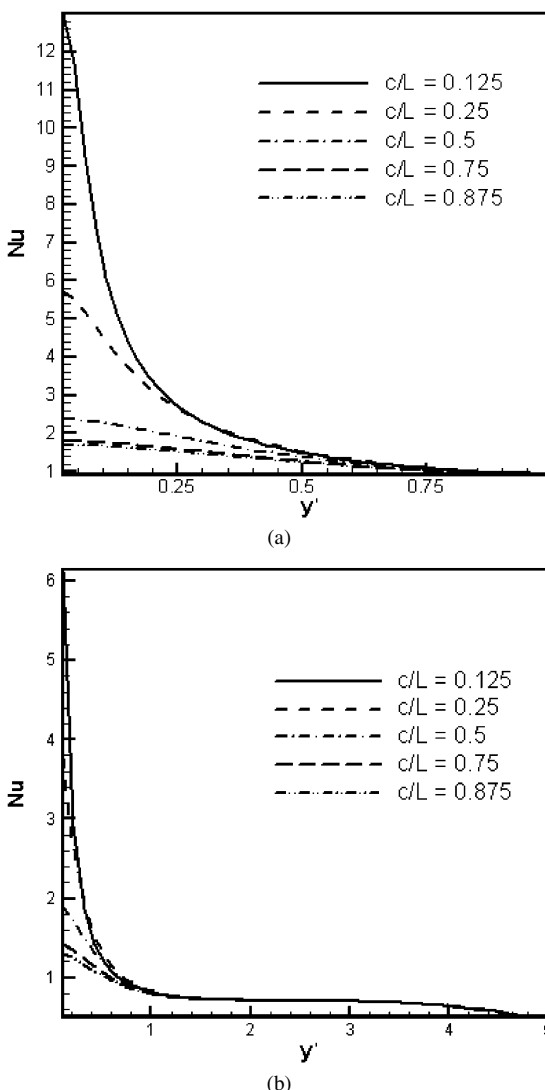


Fig. 9. Variation of local Nusselt number along the hot wall at $w/L = 0.25$, $\phi = 60^\circ$ and $Ra = 10$ (a) $A = 1$, (b) $A = 5$.

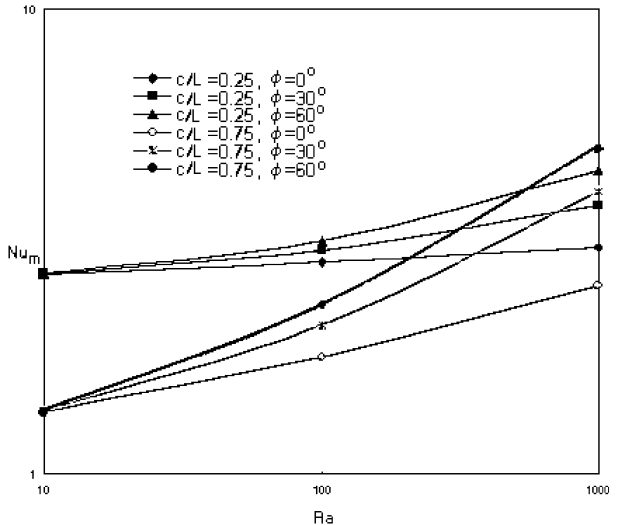


Fig. 10. Mean Nusselt number vs Rayleigh number for different locations of the cooler for $A = 1$.

When Figs. 9(a) and (b) compared, higher value of local Nusselt number is obtained for the smaller value of aspect ratio. Fig. 10 depicts the mean Nusselt number to see the effect of location of cooler. As can be seen that the value of Nusselt number is higher for $c = 0.25$ which means that cooler is near the heated wall according to far from the wall mode. There is interesting observation occurs in this case that heat transfer has the highest value for the case of $\phi = 60^\circ$ for $c = 0.75$ whereas this value can be seen for $\phi = 30^\circ$ when $c = 0.25$.

5. Conclusions

Flow field and heat transfer characteristics have been analyzed numerically for the laminar natural convection in a partially cooled and inclined rectangular porous enclosure. Finite volume based finite difference method was used with SIMPLE algorithm. Based on the obtained results in the present study, findings can be listed as follows:

- (1) Heat transfer is increased with the increasing of Rayleigh number for all parameters which governing on flow and temperature field.
- (2) Due to the partially cooler plume-like flow does not exist for all cases on the contrary of partially heating mostly studied in the literature.
- (3) Inclination angle is the dominant parameter on fluid flow and heat transfer. It causes the multicellular flow especially for square enclosure. Maximum heat transfer is obtained at $\phi = 30^\circ$.
- (4) Aspect ratio also affects the heat transfer and fluid flow. Heat transfer is decreased with the increasing of aspect ratio. For the highest value of aspect ratio, flow becomes stagnant at the far from the heated wall.
- (5) It may be an optimum solution contains all parameters but it is out of the scope of this study. However, the study can be extended in the future for instability analysis.

References

[1] D.A. Nield, A. Bejan, *Convection in Porous Media*, Springer, New York, 1992.

[2] D.B. Ingham, I. Pop (Eds.), *Transport Phenomena in Porous Media*, Elsevier, Amsterdam, 1998.

[3] K. Vafai, Convective and heat transfer in variable-porosity media, *J. Fluid Mech.* 147 (1984) 233–259.

[4] A.C. Baytas, I. Pop, Free convection in oblique enclosures filled with a porous medium, *Int. J. Heat Mass Transfer* 42 (1999) 1047–1057.

[5] A. Bejan, Flows in environmental fluids and porous media, *Int. J. Energy Res.* 27 (2003) 835–846.

[6] V. Prasad, F.A. Kulacki, Convective heat transfer in a rectangular porous cavity-Effect of aspect ratio on flow structure and heat transfer, *J. Heat Transfer* 106 (1984) 158–165.

[7] M. Sen, P. Vasseur, L. Robillard, Multiple steady states for unicellular natural convection in an inclined porous layer, *Int. J. Heat Mass Transfer* 30 (1987) 2097–2113.

[8] A.C. Baytas, I. Pop, Free convection in a square porous cavity using a thermal nonequilibrium model, *Int. J. Thermal Sci.* 41 (2002) 861–870.

[9] P. Nithiarasu, K.N. Seetharamu, T. Sundararajan, Natural convective heat transfer in a fluid saturated variable porosity medium, *Int. J. Heat Mass Transfer* 40 (1997) 3955–3967.

[10] S.L. Moya, E. Ramos, M. Sen, Numerical study of natural convection in a tilted rectangular porous material, *Int. J. Heat Mass Transfer* 30 (1987) 741–756.

[11] Al-Amiri, Natural convection in porous enclosures: The application of the two-energy equation model, *Numer. Heat Transfer A* 41 (2002) 817–834.

[12] G. Lauriat, V. Prasad, Non-Darcian effects on natural convection in a vertical porous enclosure, *Int. J. Heat Mass Transfer* 32 (1989) 2135–2148.

[13] N.H. Saeid, I. Pop, Non-Darcy natural convection in a square cavity filled with a porous medium, *Fluid Dyn. Res.* 36 (2005) 35–43.

[14] B. Farouk, T. Fusegi, Natural convection of a variable property gas in asymmetrically heated square cavity, *J. Thermophysics* 3 (1989) 85–87.

[15] T.Y. Chu, C.E. Hickox, Thermal convection with large viscosity variation in an enclosure with localized heating, *J. Heat Transfer* 112 (1990) 388–395.

[16] H.F. Oztop, I. Dagtekin, M. Duranay, Analysis of natural convection problem in a partially heated and rectangular block inserted cavity, in: Proceedings of 13th National Heat Science Conference, 2001, Turkey, pp. 217–222 (in Turkish).

[17] H.F. Oztop, Natural convection heat transfer in a partially heated square cavity with internal heat generation, in: Proceedings of 2nd International Exergy, Energy and Environment Symposium (IEEES-2), Kos-Greece, 2005.

[18] O. Aydin, W.J. Yang, Natural convection in enclosures with localized heating from below and symmetrical cooling from sides, *Int. J. Numer. Methods Heat Fluid Flow* 10 (2000) 518–529.

[19] H. Turkoglu, N. Yucel, Effect of heater and cooler locations on natural convection in square cavities, *Numer. Heat Transfer A* 27 (1995) 351–358.

[20] H.H.S. Chu, S.W. Churchill, C.V.S. Patterson, The effect of heater size, location, aspect ratio, and boundary conditions on two-dimensional, laminar, natural convection in rectangular channels, *J. Heat Transfer* (1976) 194–201.

[21] V. Prasad, F.A. Kulacki, Natural convection in horizontal porous layers with localized heating from below, *J. Heat Transfer* 109 (1987) 795–798.

[22] M.M. El-Refae, M.M. Elsayed, N.M. Al-Najem, A.A. Noor, Natural convection in partially cooled tilted cavities, *Int. J. Numer. Methods Fluids* 28 (1998) 477–499.

[23] M. Bourich, M. Hasnaoui, A. Amahmid, Double-diffusive natural convection in a porous enclosure partially heated from below and differentially salted, *Int. J. Heat Fluid Flow* 25 (2004) 1034–1046.

[24] R.L. Frederick, On the aspect ratio for which the heat transfer in differentially heated cavities is maximum, *Int. Comm. Heat Mass Transfer* 26 (1999) 549–558.

[25] P. Vasseur, M.G. Satish, L. Robillard, Natural convection in a thin, inclined, porous layer exposed to a constant heat flux, *Int. J. Heat Mass Transfer* 30 (1987) 537–549.

[26] M.A. Hossain, D.A.S. Rees, Natural convection flow of a viscous incompressible fluid in a rectangular porous cavity heated from below with cold sidewalls, *Heat Mass Transfer* 39 (2005) 657–663.

[27] L. Robillard, C.H. Wang, P. Vasseur, Multiple steady states in a confined porous medium with localized heating from below, *Numer. Heat Transfer* 13 (1988) 91–110.

[28] A. Nakayama, *PC-Aided Numerical Heat Transfer and Convective Flow*, CRC Press, Boca Raton, FL, 1995.

[29] S. Ergun, Fluid flow through packed columns, *Chem. Engrg. Prog.* 48 (1952) 89–94.

[30] S.V. Patankar, *Numerical Heat Transfer and Fluid Flow*, Hemisphere, New York, 1980.

[31] A. Narasimhan, J.L. Lage, Forced convection of a fluid with temperature-dependent viscosity flowing through a porous medium channel, *Numer. Heat Transfer A* 40 (2001) 801–820.

[32] N.H. Saeid, I. Pop, Transient free convection in a square cavity filled with a porous medium, *Int. J. Heat Mass Transfer* 47 (2004) 1917–1924.

[33] A.C. Baytas, Entropy generation for natural convection in an inclined porous cavity, *Int. J. Heat Mass Transfer* 43 (2000) 2089–2099.